

1

2 **Synthesis, characterization and cytotoxic activity of**

3 **N-(5-indanyl(methylene)anthranilic acid(5-indanyl methylene)-hydrazide and its**

4 **Pt(II) complex**

5

6

7 **Abstract** Since the discovery of the platinum based complex, cisplatin, medicinal inorganic
8 chemistry has attracted much more attention and a large number of platinum complexes with
9 promising pharmacological properties have been synthesized. In this work a new platinum complex
10 of N-(5-indanyl(methylene)anthranilic acid(5-indanyl methylene)-hydrazide (HL) has been
11 synthesized and characterized by physical and spectral techniques, as elemental analysis, IR, EI-
12 MS, ¹H-NMR, thermal analysis, transmittance electron microscope (TEM) and magnetic moment.
13 The results indicated that the ligand binds to Pt(II) in the enol form. Square-planar stereochemistry
14 was suggested for the Pt(II) complex. The morphological characterization showed nano-sized
15 spherical particles with average size 92 nm of the isolated complex. The synthesized Pt(II) complex
16 exhibited a significant cytotoxic activity against HCT116 and HEPG2. Also *in vivo* study of the
17 Pt(II) complex showed cytotoxic activity towards Ehrlich ascites carcinoma (EAC).

18 **Keywords** Synthesis. Pt(II) complex. Cytotoxic activity

19 _____

20

21 **Introduction**

22 Cancer is the major serious problem which causes death all over the world. The cause of cancer is
23 attributed to genetic damage to the cells. The damaged cells do not respond to normal tissue
24 controls. The affected cells multiply rapidly to cause spread of cancer and formation of varying
25 degrees of tumors (Zhukova and Dobrynin, 2001).

26 The discovery of effective new cancer therapies is a strong demand. Since the discovery of the
27 platinum based complex, cisplatin, in 1965 (Divsalar et al., 2013), medicinal inorganic chemistry
28 has attracted much more attention and a large number of platinum complexes with promising
29 pharmacological properties have been synthesized (Kostova, 2006). The cytotoxic action
30 mechanism of many metal complexes has been discussed aiming to develop new anti-tumor agents
31 (Grunicke et al., 2006; Noordhui et al., 2008; Chang et al., 2015; Wei et al., 2014, Sönmez M. et al.,
32 2010). The presence of metal centers capable of binding to negatively charged bio-ligands, as
33 proteins and nucleic acids offers the metal complexes excellent potential pharmaceutical properties
34 (Sakurai et al., 2002; Jian et al., 2010). The metal complex is considered a chemotherapeutic agent

35 in cancer treatment, when it slows and stops the cancer from spreading by killing the rapidly
36 dividing cells. In chemotherapy, the target is to kill the tumor cells, without causing damage to the
37 healthy cells. Cisplatin and carboplatin have been used in the treatment of various cancers as
38 chemotherapeutic agents (Kostova, 2006). Serious side effects accompany the use of these drugs,
39 so, trials are done to find new platinum complexes with less toxicity, to be used as potential anti-
40 cancer agents (Ehrsson et al., 2002). As a result, new platinum complexes with different organic
41 ligands have been designed (Al Jibori et al., 2014; Tabrizi and Chiniforoshan, 2017., Wang et al.,
42 2015; Wang et al., 2017).

43 In this paper a new Pt(II) complex of a hydrazide derivative N-(5-indanyl(methylene)anthranilic
44 acid (5-indanyl methylene)-hydrazide has been synthesized and characterized by various
45 techniques. The cytotoxic effect of the synthesized Pt(II) complex was studied.

46 To the best of our knowledge no work has been carried out on the present ligand, only a patent
47 described the synthesis, the anti-inflammatory and analgesic activity of similar derivatives
48 N-(substituted-naphthyl-1) anthranilic acid, was presented (Fujio and Tomoaki 1976).

49 **Materials and methods**

50 N-(5-indanyl(methylene)anthranilic acid(5-indanyl methylene)-hydrazide and PtCl₂ were
51 purchased from Sigma-Aldrich (S512095). ¹H-NMR of the ligand in DMSO-*d*₆ δ (ppm): 2.0 (m,
52 2H, CH₃), 2.49 (t, 4H, C₅-2H), 2.8 (t, 2H, 2H). CH=N appears at 6.8 (s, 1H), 7.43-7.8 (m, 10H).

53 **Instruments**

54 The elemental analysis, C, H and N were carried in the instrumentation center, Granada University,
55 Spain, on Thermo Scientific Flash 2000 Analyzer. TGA (thermo-gravimetical analysis
56 measurements) were carried out on a Shimadzu model 50 H instrument with nitrogen flow rate 20
57 cm³/min., and heating rate 10 °C/min. Magnetic measurements were carried out on a Sherwood
58 Scientific Magnetic Balance. The ¹H-NMR spectra in DMSO-*d*₆ were carried out on a 500 MHz
59 JEOL spectrophotometer. Fourier-transformer infrared spectra (FT-IR) were carried out as KBr
60 discs on a Mattson 5000 FTIR spectrometer. EI-MS was recorded on spectrometer WATERS
61 modelo SYNAP G2 in instrumentation center, Granada University, Spain. CM 20 PHILIPS electron
62 microscope was used to take the transmittance electron microscope (TEM) images.

63 **Synthesis of Pt(II) complex**

64 0.001 M (0.265 gm) of PtCl₂ in 10 ml ethanol was injected to 0.001 M (0.40 gm) of (N-(5-
65 indanyl(methylene)anthranilic acid (5-indanyl methylene)-hydrazide in 25 ml hot ethanolic solution
66 under nitrogen. A yellow precipitate was formed on reflux. The reaction mixture was refluxed for 3
67 hrs and the precipitate was filtered off under vacuum.

68 The trials to obtain a single crystal from the platinum complex was failed.
69 Yellow powder (yield 55%); m.p. >300 °C. Anal. Calc. for PtC₅₄H₅₇N₆O_{6.5}: C, 59.6; H, 5.3; N, 7.7;
70 Pt, 17.9% Found: C, 60.0; H, 5.4; N, 7.3; Pt, 18.1 %.

71 **Pharmacological testing**

72 *In vitro study (Cytotoxicity)*

73 Cytotoxic activity of Pt(II) was performed on a panel of human tumor cell line HEPG2
74 (hepatocellular carcinoma), HCT 116 (human colon cancer) at different concentrations. The
75 method of Philp et al was used to carry out the cytotoxicity as sulphorhodamine-B(SRB) assay
76 (Philips *et al.*, 1990). SRB is a protein stain in mild acidic conditions. This stain is used to provide a
77 sensitive index of cellular protein content. It is a bright pink amnoxanthrene dye with two
78 sulphonic groups.

79 *In vivo study (Toxicity studies)*

80 LD50 of Pt(II) complex in mice was determined according to the method of Meier and Theakston
81 (Meier and Theakston 1986).

82 *Dose response*

83 Dose response of Pt(II) complex was determined in mice according to the method described by
84 Crump et al (Crump *et al.*, 1976). Animal care and experiments were performed in accordance with
85 NIH guide to the care and use of laboratory animals.

86 Experimental design: 20 female Swiss albino mice were divided into two groups (10 mice per each
87 group): Group I is the positive control and injected intraperitoneally with 2.5x10⁶ of Ehrlich ascites
88 carcinoma "EAC" cells. Group II is the Pt(II) complex therapeutic group, injected intraperitoneally
89 with 2.5x10⁶ of Ehrlich ascites carcinoma "EAC" cells, and after one day of EAC injection,
90 therapeutic group injected intraperitoneally with 5 mg/kg of Pt(II) complex day after day. At the end
91 of the experiment, EAC cells were collected from mice and viability study was assayed.

92 *Cell viability and counting of EAC cells*

93 Trypan blue exclusion method (McLiman *et al.*, 1957) was used to determine the counting and
94 viability of EAC cells. The total and viable cells (nonstained) were determined in the two groups as
95 the number of cells /ml at magnification power X40.

96 **Statistical analysis**

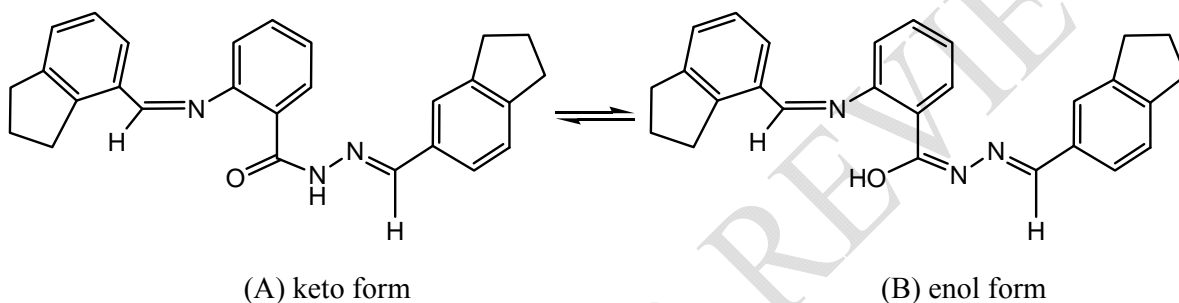
97 SPSS software version 14 (Levesquie 2007) was used to perform statistical analysis. One way
98 analysis of variance was used to assess using the effect of each parameter. The results were
99 presented as mean ± SD. Analysis of variance (ANOVA test), was used to determine the differences
100 between mean values followed by Duncan's multiple rank test using MSTAT-C computer program.

101 From linear regression analysis the statistical significance (where $P \leq 0.05$ was considered
102 significant) of the relationships between variables was calculated.

103 Results and discussion

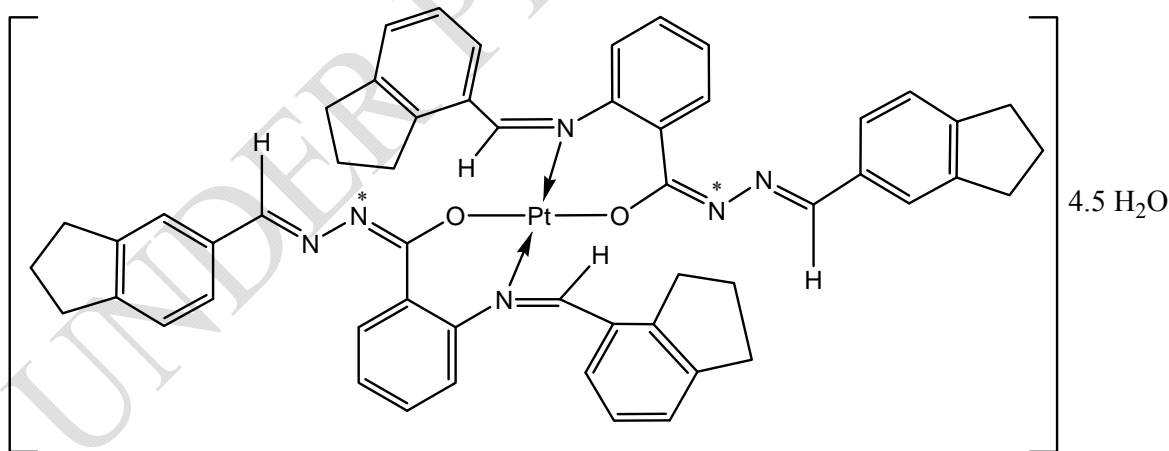
104 IR spectra of the ligand and its Pt(II) complex

105 Two tautomeric forms are suggested for the ligand, the Keto (Fig.1 A) and the enol (Fig.1B). The
106 keto form (1A) is the major tautomer in the solid state. The formula $[\text{Pt}(\text{L})_2] \cdot 4.5\text{H}_2\text{O}$ represents the
107 complex formed from the reaction of (N-(5-indanyl(methylene)anthranilic acid (5-indanyl
108 methylene)-hydrazide and PtCl_2 . The ligand chelates the Pt(II) ion in the enol form after
109 displacement of hydrogen ion from the enolic carbonyl (Fig. 2).



110
111 Fig.1. The two possible tautomeric forms of the ligand.

112 The isolated Pt(II) complex is stable in air, soluble in coordinating solvents as DMF and
113 DMSO, but insoluble in water. The elemental analysis indicated that the isolated Pt(II) complex is
114 pure compound.



115
116 Fig. 2. Suggested structure of Pt(II) complex

117 Some important IR bands of the ligand and its Pt(II) complex with their probable
118 assignments are indicated in Table 1. The ligand exhibits strong band at 3286 cm^{-1} due to $\nu(\text{NH})$.
119 The strong bands at 1662 and 1621 cm^{-1} are attributed to $\nu(\text{C}=\text{O})$ and $\nu(\text{CONH})$, respectively
120 (Nakamoto, 1970; Hosny and Sherif 2015; Hosny (2009); Hosny and Shallaby (2007). These bands

121 confirm the presence of the free ligand in the keto form. The ligand shows also, bands at 1605,
 122 1306, 1199 and 971 cm^{-1} attributed to ν (HC=N), ν (C-O), ν (C-N) and ν (N-N), respectively
 123 (Nakamoto, 1970; Hosny, 2010). Comparison of the IR spectrum of the ligand with that of Pt(II)
 124 complex reveals that the ligand chelates Pt(II) ion in a mono-negative bidentate mode *via*
 125 azomethine nitrogen (C=N) and the enolized carbonyl oxygen after displacement of hydrogen (Fig.
 126 2). The disappearance of the strong bands assigned to ν (NH), ν (CO) and ν (CONH) in the free
 127 ligand and the appearance of a new medium band at 1650 cm^{-1} assigned to ν (C=N^{*}) in the spectrum
 128 of Pt(II) complex support the suggested chelation mode. There is other possible coordination mode
 129 which may exist for the ligand, including formation of 5-membered chelate ring through N-N=CH
 130 group. This latter mode was discarded on the basis of the remaining of the bands at 969 and 1605
 131 cm^{-1} due to ν (N-N) and ν (HC=N) unaltered in comparison with its position in the spectrum of the
 132 organic ligand. The remaining of these bands unaltered, confirms the inertness of N-N active sites
 133 towards coordination (Nakamoto, 1970). The presence of hydrated water in the Pt(II) complex is
 134 confirmed by the presence of bands at 3431, 746 and 690 cm^{-1} due to ν (OH), δ (OH) and ρ_w (OH),
 135 respectively (Misbahur Rehman, 2017; Hussien et al., 2015; Hosny et al., 2014). New weak bands
 136 are observed at 557 and 449 cm^{-1} due to ν (M-O), ν (M-N) respectively (Hosny 2007; Sherif and
 137 Hosny, 2014).

138 **Table1.** IR spectral data in (cm^{-1}) for the ligand (HL) and its Pt(II) complex.

Compound	ν (NH)	ν (C=O)	ν (C=N [*])	ν (C=N)	ν (C-O)	ν (C-N)	ν (M-O)	ν (M-N)
The ligand (HL) [*]	3286	1662	-	1605	1306	1199	-	-
[Pt(L) ₂] ₃ H ₂ O	-	-	1650	1603	1292	1144	557	445

139 ^{*} HL = (N-(5-indanyl(methylene)anthranilic acid (5-indanyl methylene)-hydrazide

140 Pt(II) complex may exist either in N-N (*cis*), O-O(*cis*) or N-N(*trans*),O-O (*trans*). Molecular
 141 mechanics method was used to predict rapidly the geometries of the two suggested conformers by
 142 using hyperchem series of programs (Hyperchem 7, 2002). The total energy calculations of the two
 143 structures indicated that the *trans* form is only 2 KJ mol⁻¹ more stable than the *cis* form.

144 ¹H-NMR

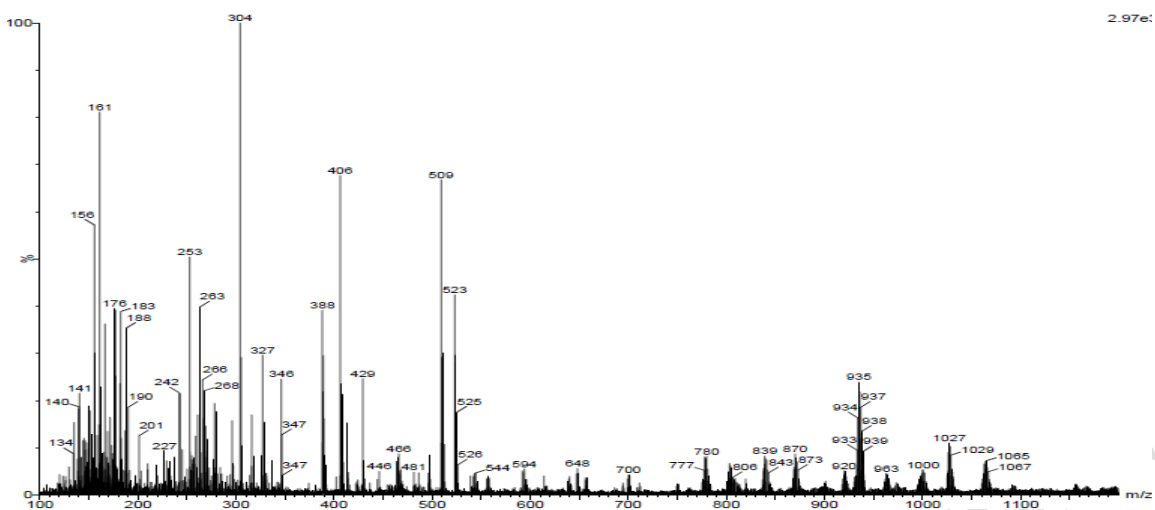
145 ¹H-NMR spectrum of the ligand (N-(5-indanyl(methylene)anthranilic acid (5-indanyl methylene)-
 146 hydrazide in DMSO-d₆ shows signals attributed to cyclopentane ring at δ 1.92-1.99 (m, 4H, 2CH₂)
 147 and 2.75-2.86 (m, 16H, 6CH₂, 4CH) (Dezső et al; 2001). Three singlet signals appear at δ 6.42,
 148 7.55, 8.73 ppm due to the protons of secondary amine NH and two azomethine protons (CH=N) and

149 CH=N-NH, respectively (Gołębiewski and Cholewińska 2004). The multiplet signals integrated for
150 6 protons resonate around 6.75 and 7.29-7.54 ppm characteristic for cyclohexadiene olefinic
151 protons. The four aromatic protons of the benzene ring are observed in the region 7.13-7.27(m, 2H,
152 Ar-H) and (m, 2H, Ar-H) (Gołębiewski and Cholewińska 2004).

153 ¹H-NMR spectrum of Pt(II) complex taken in DMSO-d₆ reveals beside the expected signals
154 of cyclopentane ring, cyclohexadiene olefinic protons in the range 1.99-3.80 ppm and the aromatic
155 protons in 6.70-7.50 ppm. The absence of the NH signal which appears at δ 6.42 ppm in the
156 spectrum of the free ligand was attributed to the enolization of the carbonyl with subsequent
157 liberation of this proton on coordination to the Pt(II) ion. The singlet signal of the azomethine
158 (CH=N) resonates downfield at δ 8.00 ppm. This shift in the signal position supports the
159 participation of the azomethine group in complex formation.

160 **Mass spectra**

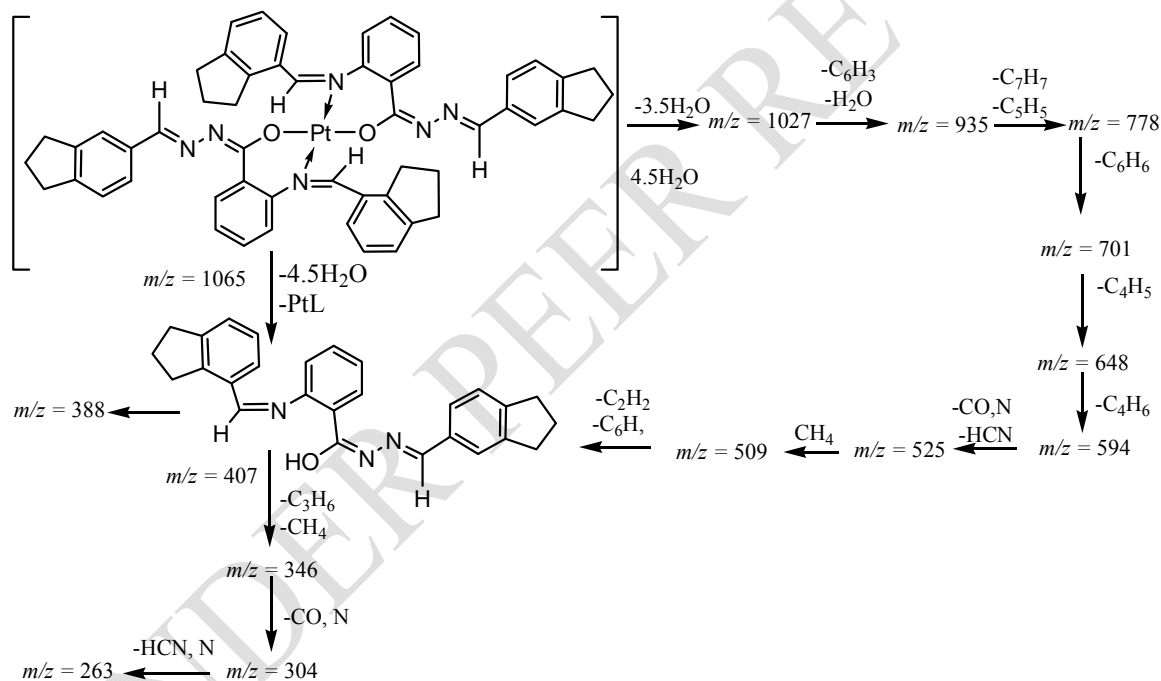
161 The EI-MS of Pt(II) complex (Fig. 3) exhibits the molecular ion peak at $m/z = 1087$, in agreement
162 with the formula $[\text{Pt}(\text{C}_{27}\text{H}_{23}\text{N}_3\text{O})_2]4.5\text{H}_2\text{O}$ after removal of H_2 . Two possible pathways have been
163 suggested for the fragmentation of Pt(II) complex (Scheme 1). The molecular ion peak may lose
164 four and half water molecules and the fragment $[\text{PtL}]$ to give a peak at $m/z = 406$, assigned to the
165 free ligand. The free ligand is fragmented by loss of propene and methane molecule by special
166 rearrangement to give the peak at $m/z = 346$. The last peak is further fragmented by loss of carbon
167 monoxide and nitrogen giving the base peak at $m/z = 304$. The base peak loses hydrocyanic acid and
168 nitrogen forming the peak at $m/z = 263$. In the second pathway, it was suggested that the molecular
169 ion peak loses three and half molecules of water forming the peak at $m/z = 1027$. The latter peak is
170 fragmented by lose of water molecule and the fragment C_6H_3 giving the peak at
171 $m/z = 935$. The latter peak loses tropyllium and furayl groups to give the peak at $m/z = 778$. The
172 peak at $m/z = 778$ is further fragmented by loss of benzene and butadiene to give the peaks at $m/z =$
173 701 and 648, respectively. The last fragment loses butane to produce the fragment at $m/z = 594$,
174 which loses hydrocyanic acid, carbon monoxide and nitrogen producing the fragment $m/z = 525$.
175 The last fragment at $m/z = 525$ loses methane, ethylene and benzene leading to the peak corresponds
176 to the free ligand at $m/z = 407$.



177

178 Fig. 3 . MS of Pt(II) complex

179



180

181 Scheme 1. Fragmentation pattern of Pt(II) complex

182 Magnetic measurements

183 The Pt(II) complex is diamagnetic which confirms the formation of a square–planar stereochemistry
 184 around the Pt(II) ion (Lever, 2002).

185 Thermal analysis

186 TGA measurements of Pt(II) complex were carried out from 25 °C up to 1000 °C.
 187 The thermogram exhibits three events. The first resulted from the removal of water of hydration.
 188 This step starts from 25 °C to 140 °C (Soliman et al 2005). The next step was attributed to the loss

189 of two phenyl and four benzocyclopentane rings. This step takes place from 141 °C to 480 °C.
190 (Found mass loss of this step is 55.5%, while the calculated mass loss is 57.0%). The last step starts
191 from 461 °C to 880 °C, corresponding to the loss four hydrocyanic acid molecules (Found mass loss
192 of this step is 8.7%; Calcd 9.0%).

193 The thermodynamic parameters of decomposition were calculated by applying Coats-Redfern
194 (Coats-Redfern, 1964) equations. The energy of activation (E^*) and the order of the reaction (n)
195 were determined graphically. The thermodynamic parameters E^* , ΔH^* , ΔG^* and ΔS^* were calculated
196 from equations (1-3) and found to be 10.5, 4.7, 217 KJ and -301.7 S^{-1} , respectively:

197
$$\Delta S^* = 2.303 [\log (Zh/KT)]R \quad (1)$$

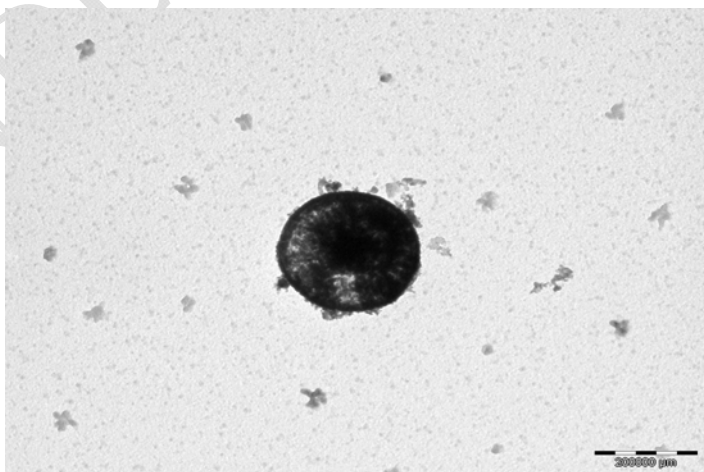
198
$$\Delta H^* = E - RT \quad (2)$$

199
$$\Delta G^* = \Delta H^* - Ts \Delta S^* \quad (3)$$

200 (Where, Z , h and K are the pre-exponential factor, Plank and Boltzmann constants, respectively
201 (Sherif and Hosny, 2014). The thermodynamic parameters were calculated for the second step,
202 which is suitable for kinetic analysis, where there is no overlapping with other steps. The positive
203 enthalpy and free energy values reveal the endothermic and non-spontaneous decomposition of this
204 step, respectively. The negative entropy value indicates that the structure of the activated complex is
205 more ordered than the reactants (Sherif and Hosny, 2014).

206 **Morphological characterization**

207 The chemical and biological activities of metal complexes were related to their particles size and
208 shape (Hussain and Chakravarty,2012; Hosny et al., 2015). Transmittance electron microscope
209 (TEM) was used to determine the particles shape and size of Pt(II) complex. From the TEM images
210 (Fig.4), it is clear that the particles of Pt(II) complex are spherical in shape.



220

Fig. 4. TEM images of Pt(II) complex

221 The possible formation mechanism of the spherical particles of Pt(Indanyl) complex has been
 222 proposed as indicated in Scheme 1. Under reflux conditions, the soluble Pt²⁺ cation reacts with the
 223 indanyl ligand to form insoluble Pt(Indanyl) nucleus. In the first stage, Pt(Indanyl) complex follows
 224 a heterogeneous nucleation, where the energy barrier is lower than nucleation in solution (Luo et al.,
 225 2011; Mohammadikish 2014). Initially, large numbers of small primary nanoparticles are formed.
 226 These primary particles have high surface energy, which makes them unstable. They aggregate
 227 rapidly and grow forming spherical nanoparticles. The nanospheres are assembled to each other via
 228 random attachment to reduce the surface energy forming thermodynamically stable structure.
 229 Finally, spontaneous aggregation takes place in spherical form to minimize the surface area.

230 **Biological Study**

231 *Cytotoxicity*

232 The in vitro cytotoxic activities of Pt(II) and the standard doxorubicin were shown in Table 2 and
 233 Figs 5, 6. The minimum inhibitory concentration of the synthesized compound was found to be 5.3
 234 µg/ml and 9.68 µg/ml against HCT116 and HEPG2 cell lines, respectively. The colorimetric
 235 cytotoxicity tests showed that the Pt(II) complex has in vitro cytotoxic activity against the examined
 236 cancerous cell lines with IC₅₀ values of 9.08 µM and 5.43 µM against HCT116 and HEPG2 cell
 237 lines, respectively. The current results revealed that the present Pt complex inhibits cell proliferation
 238 in the same range as cisplatin and oxaliplatin.

239 **Table 2.** Minimum inhibitory concentration of doxorubicin and synthesized Pt(II) complex against
 240 HCT116 and HEPG2 cell lines

	HCT116	HEPG2
Doxorubicin	5.3 µg/ml	5.18 µg/ml
Pt (II) complex	9.68 µg/ml	5.78 µg/ml

241

242 *Determination of median lethal dose (LD50) of Pt(II) complex*

243 The results revealed that, dose up to 100 mg/kg body weight was considered safe, where no
 244 mortality was observed. Table 3 summarizes the effect of Pt(II) complex on EAC cells volume and
 245 count.

246

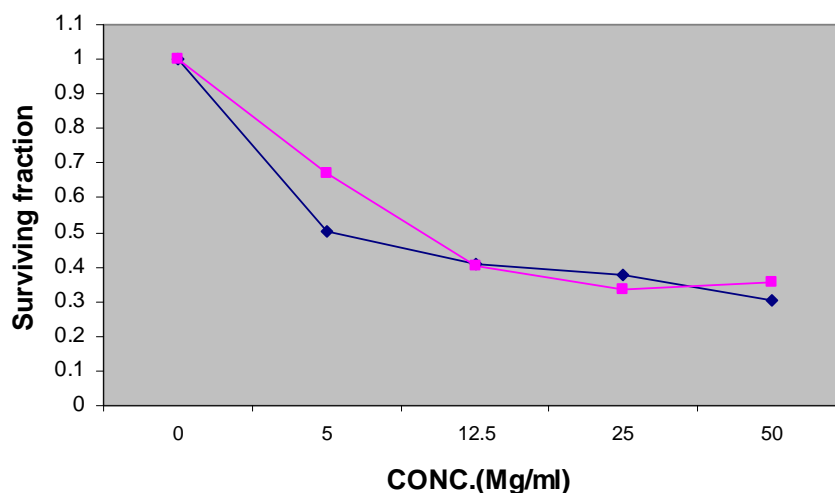
247 **Table 3.** Effect of Pt (II) complex on the volume and count of EAC in the studied groups:

Parameter	Positive control	Pt(II) complex
Volume of Ascites fluid(ml)	3.9 ± 0.11	2.24±0.18

% change	-	42.56%
Count of EAC cells ($\times 10^6$)	55.4 ± 0.32	26.3 ± 0.64
% change	-	52.53%

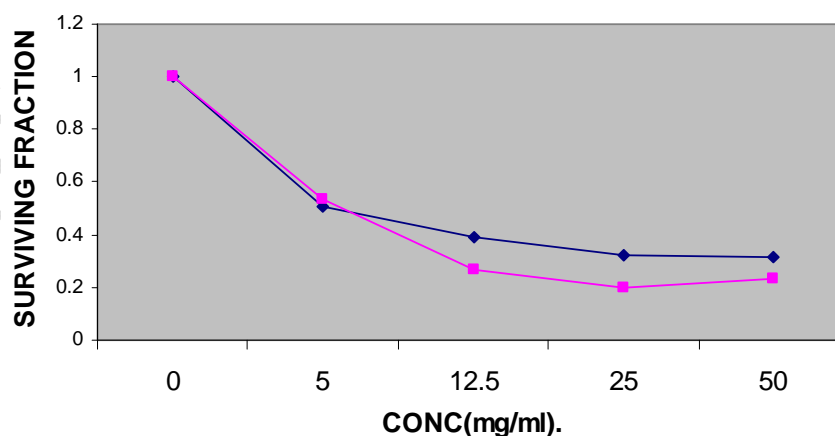
248

249 The results indicate mean volume of EAC of the positive control group is 3.9 ml. This value was
 250 significantly decreased by 42.5% in Pt(II) complex treated group ($P < 0.05$). Also, it was found that
 251 the mean count of EAC cells in the positive control group is 55.4×10^6 which was significantly
 252 decreased in Pt(II) complex treated group, compared to the positive control group.



253

254 Fig. 5. Minimum inhibitory concentration of Pt(II) complex (pink) and doxorubicin (blue) against
 255 HCT cell line



256

257 Fig. 6. Minimum inhibitory concentration of Pt(II) complex (pink) and doxorubicin (blue) against
 258 HEPG2T cell line

259 **Conclusion**

260 To the best of our knowledge no work has been carried out on the ligand
261 N-(5-indanyl(methylene)anthranilic acid(5-indanyl methylene)-hydrazide and its metal complexes.
262 The Pt(II) complex of this ligand has been synthesized and characterized by different techniques.
263 The ligand coordinates to the Pt(II) ion in the enol form as mono-negative bidentate forming
264 square-planar complex. TEM images indicated that the particles of Pt(II) complex exist as spherical
265 nanoparticles. The Pt(II) complex exhibits activities on four human cancer cell lines HEPG2
266 and HCT 116 with $IC_{50} = 1.4-9.6 \mu M$. The activity of the Pt(II) complex was compared with some
267 standard platinum complexes as cisplatin and carboplatin complexes.

268
269 **References**

270 **Al-Jibori S. A.**, Al-Jibori G. H., Al-Hayaly L. J., Wagner C., Schmidt H., Timur S., Barlas F. B.,
271 Subasi E., Ghosh S., Hogarth G. 2014. Combining anti-cancer drugs with artificial sweeteners:
272 Synthesis and anti-cancer activity of saccharinate (sac) and thiosaccharinate (tsac) complexes *cis*-
273 $[Pt(sac)_2(NH_3)_2]$ and *cis*- $[Pt(tsac)_2(NH_3)_2]$, *Journal of Inorganic Biochemistry*, 141: 55.
274 [doi:10.1016/j.jinorgbio.2014.07.017](https://doi.org/10.1016/j.jinorgbio.2014.07.017)

275 **Coats A. W.**, Redfern J. P. (1964) Kinetic parameters from thermogravimetric. *Nature*, 201:68.
276 [doi:10.1038/201068a0](https://doi.org/10.1038/201068a0)

277 **Crump K. S.**, Hoel D. G., Langley C. H., Peto R. 1976. Fundamental carcinogenic processes and
278 their implications for low dose risk assessment. *Cancer Research*, 36:2973.
279 [doi: Published September 1976](https://doi.org/10.1056/NEJM197609133617a01)

280 **Dezső G.**, Evanics F., Dombi G., Bernáth G. 2001. 1H and ^{13}C NMR Chemical shift assignments of
281 a cyclopentane-fused *cis*-azetidinone (*cis*-azabicyclo[3.2.0]heptan-7-one). *Atheoretical and*
282 *experimental investigation. ARKIVOC* III: 73.

283 **Divsalar A.**, Zhila I., Saboury A. A., Nabiuni M., Razmi M., Mansuri-Torshizi H. 2013. Cytotoxic
284 and spectroscopic studies on binding of a new synthesized bipyridine ethyl dithiocarbamate Pt(II)
285 nitrate complex to the milk carrier protein of BLG. *Journal of Iranian Chemical Society*, 10: 951.
286 DOI 10.1007/s13738-013-0232-6

287 **Ehrsson H.**, Wallin I., Yachnin J. 2002. Pharmacokinetics of oxaliplatin in humans. *Medical*
288 *Oncology*, 16: 261. [doi:10.1385/MO:19:4:261](https://doi.org/10.1385/MO:19:4:261)

- 289 **Foltinova V.**, Svihalkova L. S., Horvath V., Sova P., Hofmanova J., Janisch R., Kozubík A. 2008.
290 Mechanism of effects of Pt(II) and (IV) complexes. Comparison of cis platin and oxaliplatin with
291 satraplatin and LA-12, new platinum (IV) based drugs. A mini review. *Scripta Medica (BRNO)*,
292 81:105.
- 293 **Fujio N.**, Tomoaki F. 1976. Substituted naphthyl anthranilic acids. *United States Patents*,
294 3989746A.
- 295 **Golebiewski M.**, Cholewińska M. 2004. Synthesis and spectral studies of transition metal
296 complexes of aryloylhydrazones of 5- methylsalicylaldehyde, *Pestycydy*, 1-2: 21.
- 297 **Grunicke H.**, Doppler W., Helliger W. 1986. Tumor biochemistry as basis for advances in tumor
298 chemotherapy. *Archive Geschwulstforsch*, 156:193. [PMID:3488047](#)
- 299 **Hosny N. M.** 2007. Synthesis, characterization, theoretical calculations and catalase-like activity of
300 mixed ligand complexes derived from alanine and 2-acetylpyridine. *Transition Metal Chemistry*,
301 32: 117. [doi: 10.1007/s11243-006-0132-z](#)
- 302 **Hosny N. M.** 2009. Synthesis and Characterization of Transition Metal Complexes Derived from
303 (E)-(N)-(1-(Pyridine-2-yl)ethylidene)benzohydrazide (PEBH). *Journal Molecular Structure*,
304 923:98. [doi.org/10.1080/15533174.2011.591296](#)
- 305 **Hosny N. M.** 2010. Cu(II) and Zr(IV) Complexes with (E)-N-(1-(Pyridine-4-
306 yl)ethylidene)nicotinohydrazide. *Synth. React. Inorg-Org Met Nano* 6: 391.
307 [doi:10.1080/15533174.2010.492550](#)
- 308 **Hosny N. M.**, El Morsy E. A., Sherif Y. E. 2015. Synthesis, spectral, optical and anti-inflammatory
309 activity of complexes derived from 2-aminobenzohydrazide with some rare earths.
310 *Journal of Rare Earths*, 33: 758. [doi.org/10.1016/S1002-0721\(14\)60482-8](#)
- 311 **Hosny N. M.**, Hussien M. A., Radwan F. M., Nawar N. 2014. Synthesis, spectral characterization
312 and DNA binding of Schiff-base metal complexes derived from 2-amino-3-hydroxypropanoic acid
313 and acetylacetone. *Spectrochimica Acta A*, 132: 121. [doi:10.1016/j.saa.2014.04.165](#)
- 314 **Hosny N. M.**, Shallaby A. M. 2007. Spectroscopic Characterization of Some Metal Complexes
315 Derived from 4-Acetylpyridine Nicotinoylhydrazone, *Transition Metal Chemistry*, 32:1085. [Doi: 10.1007/s11243-007-0288-1](#)
- 317 **Hosny N. M.**, **Sherif Y. E.** 2015. Synthesis, structural, optical and anti-rheumatic activity of
318 metal complexes derived from (E)-2-amino-N-(1-(2-aminophenyl)ethylidene) benzohydrazide (2-

319 AAB) with Ru(III), Pd(II) and Zr(IV). *Spectrochimica Acta A*, 136:510.
320 doi.org/10.1016/j.saa.2014.09.064

321 **Hussain J., Chakravarty A. R.** 2012. Photocytotoxic lanthanide complexes, *Journal of Chemical*
322 *Science*, 124:1327.

323 **Hussien M. A., Nawar N., Radwan F. M., Hosny N. M.** 2015. Spectral characterization, optical
324 band gap calculations and DNA binding of some binuclear Schiff-base metal complexes derived
325 from 2-amino-ethanoic acid and acetylacetonate, *J. Mol. Struct.*, 1080:162.
326 doi.org/10.1016/j.molstruc.2014.09.071

327 **Hyperchem 7**, developed by Hypercube Inc. 2002.

328 **Jain A., Jain S. K., Ganesh N.** 2010. Design and development of ligand-appended polysaccharidic
329 nanoparticles for the delivery of oxaliplatin in colorectal cancer, *Nanomedicine Nanotechnology*
330 *Biology and Medicine*, 6: 179. DOI:[10.1016/j.nano.2009.03.002](https://doi.org/10.1016/j.nano.2009.03.002)

331 **Kostova I.** 2006. Platinum complexes as anticancer agents, *Recent Patents on Anti-Cancer Drug*
332 *Discovery*, 1:1.

333 **Lever A. B. P.** 1986. Inorganic electronic spectroscopy, Elsevier, Amsterdam.

334 **Levesque R.** 2007. SPSS: Programming and Data Management: A Guide for SPSS and SAS users,
335 Fourth Edition, SPSS INC, Chicago III.

336 **Luo L. J., Tao W., Hu X. Y., Xiao T., Heng B. J., Huang W., Wang H., Han H. W., Jiang Q. K.,**
337 **Wang J. B., Tan Y. W.** 2011. Mesoporous F-doped ZnO prism arrays with significantly enhanced
338 photovoltaic performance for dye-sensitized solar cells. *Journal of Power Sources*, 196: 10518.
339 doi.org/10.1016/j.jpowsour.2011.08.011

340 **McLiman W. F., Dairs E. V., Glover F. L., Rake G. W.** 1957. The submerged culture of mammalian
341 cells; the spinner culture, *Journal of Immunology*, 79:428. PMID:[13491853](https://pubmed.ncbi.nlm.nih.gov/13491853/)

342 **Meier J., Theakston R. D.** 1986. Approximate LD50 determinations of snake venoms using eight to
343 ten experimental animals. *Toxicology Journal*, 24:395. PMID:[3715904](https://pubmed.ncbi.nlm.nih.gov/3715904/)

344 **Misbah ur Rehman, Imran M., Arif M.** 2013. Synthesis, Characterization and in vitro
345 Antimicrobial studies of Schiff-bases derived from Acetylacetonate and amino acids and their
346 oxovanadium(IV) complexes. *American Journal of Applied Chemistry*, 1: 59. doi:
347 [10.11648/j.ajac.20130104.13](https://doi.org/10.11648/j.ajac.20130104.13)

348 **Mohammadikish M.** 2014. Green synthesis and growth mechanism of new nanomaterial: Zn
349 (salen) nano-complex. *Crystal Engineering Communication*,
350 16:8020.doi.org/10.1016/j.jcrysgro.2015.08.029

351 **Mujahid M.,** Kia A. F., Duff B., Egan D. A., Devereux M., McClean S., Walsh M., Trendafilova
352 N., Georgieva I., Creaven B. S. 2015. Spectroscopic studies, DFT calculations, and cytotoxic
353 activity of novel silver(I) complexes of hydroxy ortho-substituted-nitro-2H-chromen-2-one ligands
354 and a phenanthroline adduct. *Journal Inorganic*
355 *Biochemistry*,153:103.[doi:10.1016/j.jinorgbio.2015.10.007](https://doi.org/10.1016/j.jinorgbio.2015.10.007)

356 **Nakamoto K.,** (ed). (1970) Infrared spectra of inorganic and coordination compounds. John Wiley,
357 New York.

358 **Noordhui P.,** Laan A., Born K., Losekoot N., Kathmann I., Peters G. 2008. Oxaliplatin activity in
359 selected and unselected human ovarian and colorectal cancer cell lines. *Biochemical Pharmacol*
360 *ogy*, 76: 53. [doi:10.1016/j.bcp.2008.04.007](https://doi.org/10.1016/j.bcp.2008.04.007)

361

362 **Philips S.,** Rista S., Dominic S., Anne M., Jaames M., David V., Jonathan T. W., Heidi B., Susan
363 K., Michael R. B. 1990. Newcoloremtric cytotoxicity assay for anti-cancer drug screening. *Journal*
364 *of National Cancer Institute*, 8:1107. [doi:10.1016/j.bcp.2008.04.007](https://doi.org/10.1016/j.bcp.2008.04.007)

365 **Sakurai H.,** Kojima Y., Yoshikawa Y., Kawabe K., Yasui H. 2002. Antidiabetic vanadium(IV) and
366 zinc(II) complexes. *Coordination Chemistry Review*, 226: 187. [doi.org/10.1016/S0010-](https://doi.org/10.1016/S0010-8545(01)00447-7)
367 [8545\(01\)00447-7](https://doi.org/10.1016/S0010-8545(01)00447-7)

368 **Sherif Y. E.,** Hosny N. M. 2014. Synthesis, characterization, and anti-rheumatic potential of
369 phthalazine-1,4-dione and its Cu(II) and Zn(II) complexes, *Medicinal Chemistry Research*,
370 23:2536. [doi: 10.1007/s00044-013-0827-6](https://doi.org/10.1007/s00044-013-0827-6)

371 **Sherif Y. E.,** Hosny N. M. 2014. Anti-rheumatic potential of ethyl 2-(2-cyano-3-mercapto-3-
372 (phenylamino) acrylamido)-4,5,6,7-tetrahydrobenzo[b]thiophene-3-carboxylate and its Co(II),
373 Cu(II) and Zn(II) complexes, *European Journal of Medicinal Chemistry*, 83: 338.
374 doi.org/10.1016/j.ejmech.2014.06.038

375 **Soliman A. A.,** Mohamed G. G., Hosny W. M., El-Mawgood M. A. 2005. Synthesis,
376 Spectroscopic and thermal characterization of new sulfasalazine metal complexes. *Synth. React.*
377 *Inorg. Met-Org. Nano-Met.Chem.* , 35:483. DOI: [10.1081/SIM-200067043](https://doi.org/10.1081/SIM-200067043)

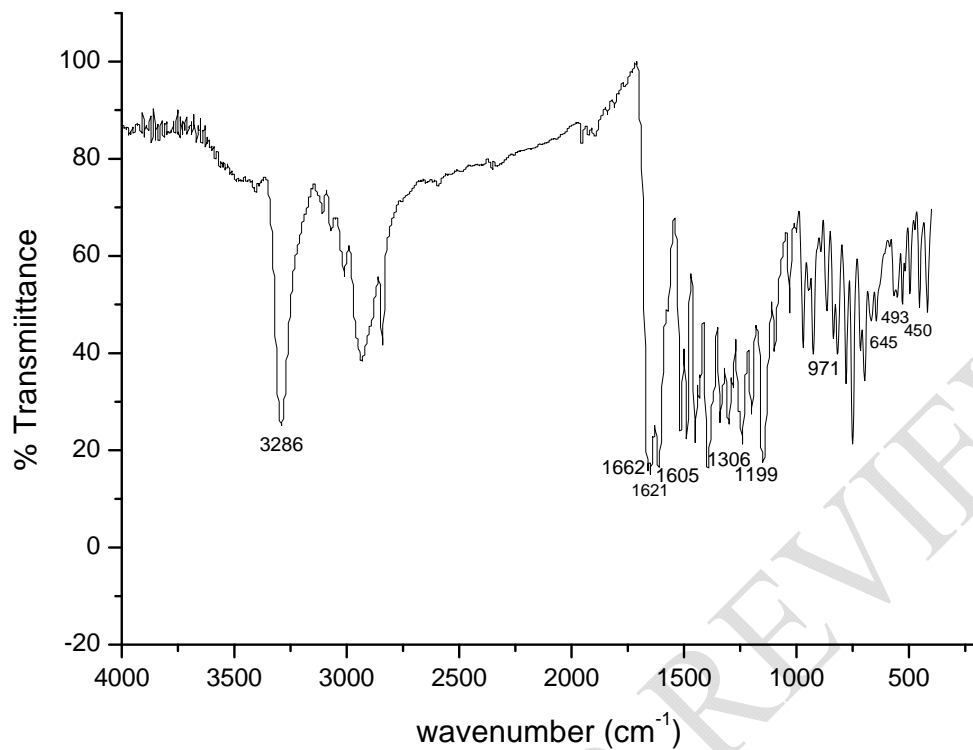
378

- 379 **Sönmez M.**, Celebi M., Yardim Y., Sentürk Z. 2010. Palladium(II) and platinum(II) complexes a
380 symmetric Schiff base derived from 2,6-diformyl-4-methylphenol with N-aminopyrimidine:
381 Synthesis, characterization and detection of DNA interaction by voltammetry, *European Journal of*
382 *Medicinal Chemistry*, 45: 4215. doi: [10.1016/j.ejmech.2010.06.016](https://doi.org/10.1016/j.ejmech.2010.06.016).
- 383 **Tabrizi L.**, Chiniforoshan H. 2017. Cytotoxicity and cellular response mechanisms of water-
384 soluble platinum(II) complexes of lidocaine and phenylcyanamide derivatives. *BioMetals*,
385 30:59. doi:[10.1007/s10534-016-9986-5](https://doi.org/10.1007/s10534-016-9986-5)
- 386 **Wang B.**, Wang Z., Ai F., Tang W. K., Zhu G. 2015. A monofunctional platinum(II)-based
387 anticancer agent from a salicylanilide derivative: Synthesis, antiproliferative activity, and
388 transcription inhibition, *Journal of Inorganic Biochemistry*. 142: 118.
389 doi.org/10.1016/j.jinorgbio.2014.10.003
- 390 **Wang Q.**, Yang L., Wu J., Wang H., Song J., Tang. X. 2017. Four mononuclear platinum(II)
391 complexes: Synthesis, DNA/BSA binding, DNA cleavage and cytotoxicity. *BioMetals*, 30:17.
392 [doi:10.1007/s10534-016-9984-7](https://doi.org/10.1007/s10534-016-9984-7)
- 393 **Zhukova O. S.**, Dobrynin I.V. 2001. Current results and perspectives of the use of human tumor
394 cell lines for antitumor drug screening. *Voprosy Onkologii*, 47: 706. PMID:11826493

395

396 Supporting Informations

397



398

399

400

Fig. S1. IR spectrum of the ligand

401

402

403

404

405

406

407

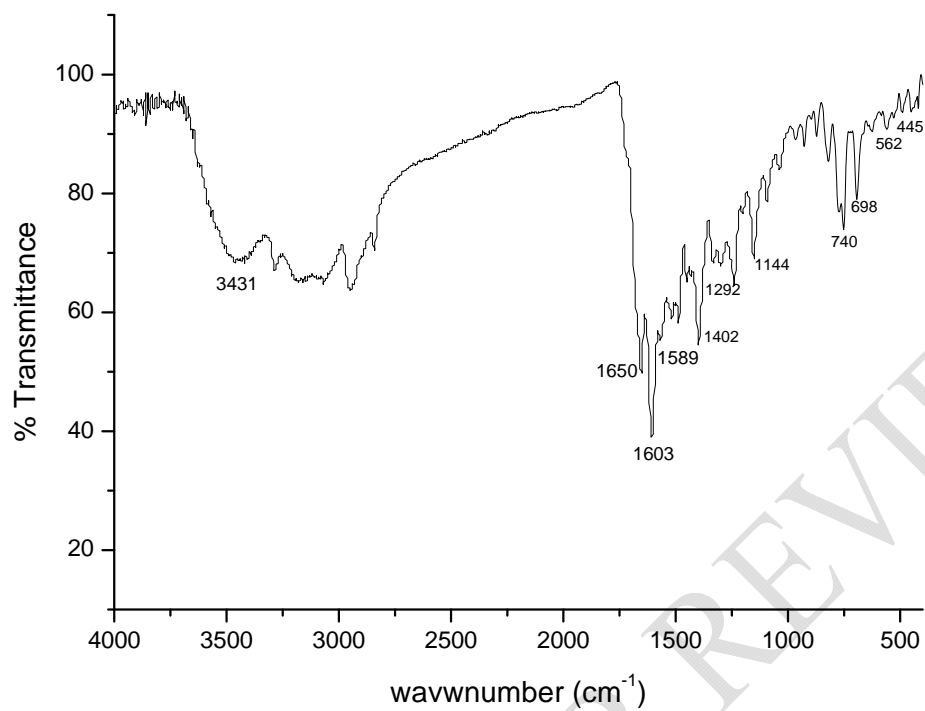
408

409

410

411

412



414

415

416 Fig. S2. IR spectrum of Pt(II) complex

417

418

419

420

421

422

423

424

425

426

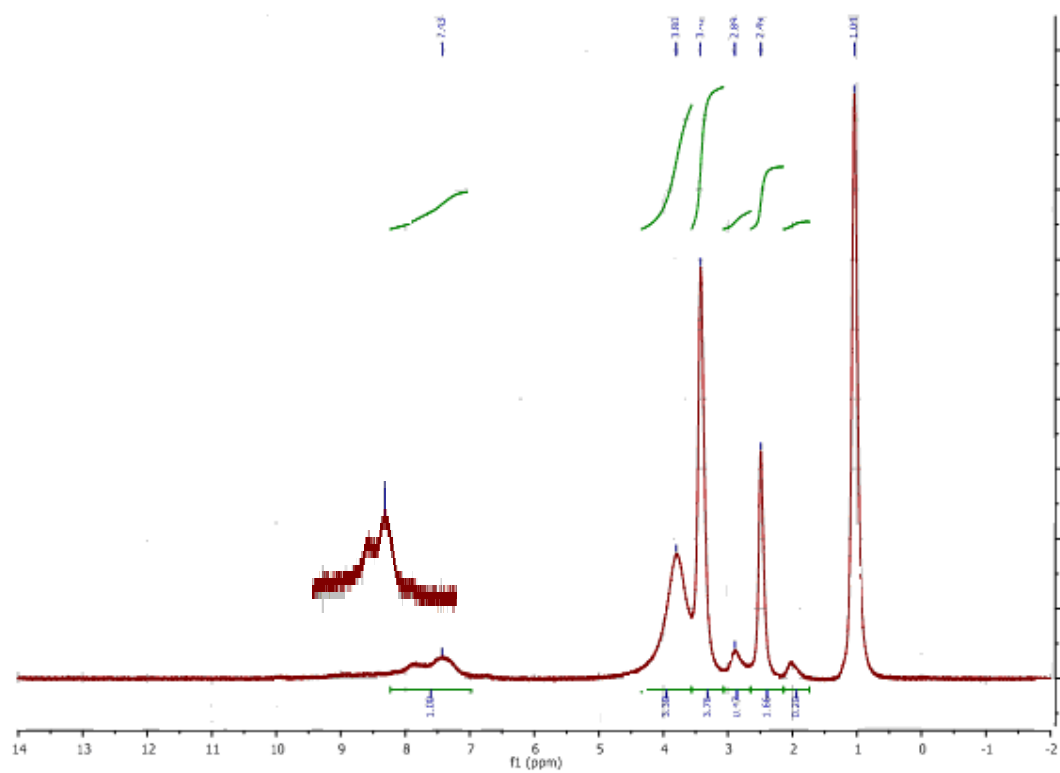
427

428

429

430

431



432

433 Fig. S3. ¹H NMR spectrum of Pt(II) complexes

434

435

436

437

438

439